Int J Adv Manuf Technol (2009) 40:503–511
DOI 10.1007/s00170-007-1355-7

ORIGINAL ARTICLE

Free abrasive wire saw machining of ceramics

C. Y. Hsu · C. S. Chen · C. C. Tsao

Received: 13 April 2007 / Accepted: 11 December 2007 / Published online: 19 March 2008

Abstract Currently, many kinds of ceramics are used in advanced industrial fields due to their superior mechanical properties, such as thermal, wear, corrosion resistance, and lightweight features. Wire saw machining ceramic (Al_2O_3) was investigated by ultrasonic vibration in this study. Taguchi approach is a powerful design tool for high-quality systems. Material removal rate, wafer surface roughness, steel wire wear, kerf width, and flatness during machining ceramic were selected as quality character factors to optimize the machining parameters (swinging angle, concentration, mixed grain and direction of ultrasonic vibration) to get the larger-the-better (material removal rate) and the smaller-the-better (wafer surface roughness, steel wire wear, kerf width and flatness) machining characteristics by Taguchi method. The results indicated that wire swinging produces a higher material removal rate and good wafer surface roughness. Ultrasonic vibration improved material removal rate, without affecting the flatness under different machining conditions. Experimental results show that the optimal wire saw machining parameters based on grey relational analysis can be determined effectively and material removal rate increases from 2.972 to 3.324 mm^2/min, wafer surface roughness decreases from 0.37 to 0.34 μm, steel wire wear decreases from 0.78 to 0.77 μm, kerf width decreases from 0.352 to 0.350 mm, and flatness decreases from 7.51 to 7.22 μm are observed.

C. Y. Hsu (✉) · C. S. Chen
Department of Mechanical Engineering,
Lunghwa University of Science and Technology,
Taoyuan 33306 Taiwan, Republic of China
e-mail: cyhsu@mail.lhu.edu.tw

C. C. Tsao
Department of Automation Engineering,
Tahua Institute of Technology,
Hsinchu 30740 Taiwan, Republic of China

Keywords Wire saw · Ultrasonic vibration-aided · Material removal rate · Ceramics

1 Introduction

Ceramics have been developed and utilized in many fields. They possess thermal, wear, and corrosion-resistance characteristics and lightweight features that metals lack. Therefore, ceramic development has a significant influence on advanced industries. Since ceramic fracture resistance is far lower than that of metals, plastic deformation during machining, often seen in machining of metals, is unlikely. Instead, a new surface marked with extended minute cracks is created resulting in a difficult control of machining precision and machined surface roughness. Therefore, increasing the machining quality and reducing the machining costs for ceramics is central for further ceramic product development.

Wire saw machining is a technique where stainless-steel wires are utilized to mobilize abrasive slurry when cutting semiconductors, crystals, various single crystals, oxide semiconductors, magnetic materials, and other brittle materials. The wire can be of single or multiple strands. Wire saw cutting has the following features: (1) low heat dissipation during machining, resulting in a small number of disturbed layers on the work surface; (2) fine kerf width (wire diameter of ≤0.3 mm) can be obtained with reduced waste materials; (3) similar to polishing, good surface roughness can be obtained under appropriate control of machining parameters [1, 2]; (4) structural rigidity requirements of wire saw machines is lower than that of conventional cutting machines.

Yamamoto utilized multiple wire saws to cut granite and achieved very good cutting efficiency [3]. Contardi proved that using wire saw to precision-cut ceramics was more

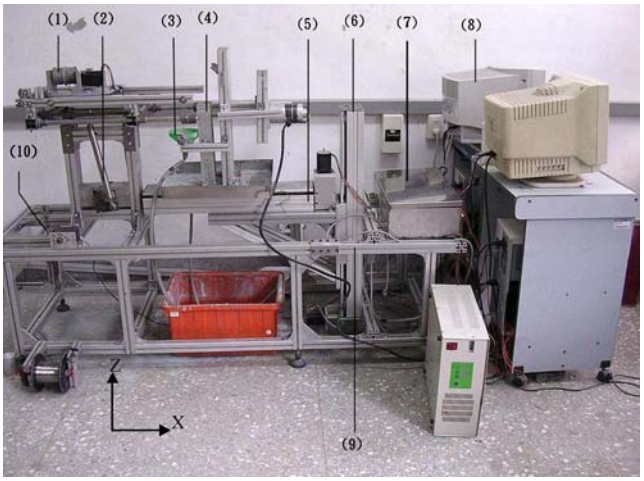

Fig. 1 Single wire saw and experimental system. *1* Steel wire reciprocating gear mechanism. *2* Steel wire swinging cutting mechanism. *3* Slurry collector. *4* Workpiece fixture and ultrasonic vibration mechanism. *5* X-axis platform. *6* Z-axis platform. *7* Control box. *8* PC-based controller. *9* Frame *10* Steel wire tension holder

economical than conventional machining approaches [4]. Kojima employed highly efficient multiple-wire saw machining, employed in precision cutting of silicon ingots into thin wafers [5]. Suwabe et al. investigated the effect of different combinations of slurry grains on wire saw machining efficiency [6]. Clark et al. machined wood and foam ceramics using fixed-abrasive diamond-wire machining [7]. Currently, inner diameter blade grinding is the major semiconductor industry approach in slicing silicon ingots. However, the current trend of increasing wafer diameter to =12 inches has made the application of inner diameter blade grinding increasingly difficult. Multiple wire saw machining under this circumstance may have a very important role.

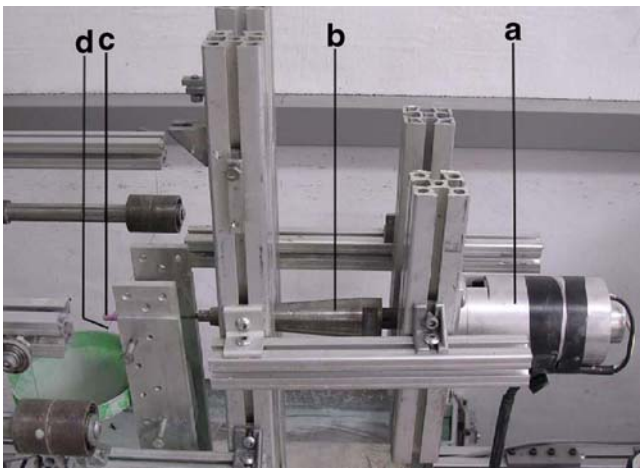

Fig. 2 Workpiece fixture and ultrasonic vibration mechanism. **a** Ultrasonic vibration perpendicular to the workpiece feeding direction; **b** Horn; **c** Workpiece; **d** Steel wire

Table 1 Experimental conditions, factors and levels

Experimental conditions			
Workpiece	Al_2O_3 (ϕ8 mm)		
Wire diameter (mm)	Stainless-steel wire ϕ0.3±0.01		
Slurry contents	GC + Water		
Wire speed (m/s)	1.67		
Wire tension (*N*)	14.7		
Experimental factors	Level 1	Level 2	Level 3
Swinging angle (1 Hz), θ	0°	17°	25°
Concentration, *C* (%wt)	20	35	45
Mixed grain, *G* (mesh)	#600+#1000	#600+#800	#600
Direction of Ultrasonic, *U* (160 Watt)	0	Parallel to the feed	Perpendicular to the feed

Machined surface roughness, kerf width, and wafer flatness are important parameters in wire saw machining quality, whereas increasing material removal rate and reducing steel wire wear are important efficiency factors in wire saw machining. Thus, this study examines machining parameter effect, such as wire swinging angle, different slurry concentrations, mixed grains and ultrasonic vibration on machining characteristics, such as material removal rate, machined surface roughness of wafer, kerf width, steel wire wear, and flatness.

2 Experimental design

Figure 1 presents the single wire saw setup utilized in the experiment. The operating mechanism for wire saw machining is discussed in the following text. The gear mechanism provides the drive for reciprocating steel wire movement (*1* in Fig. 1) while holding steel wire tension (*10* in Fig. 1). A stepping motor is controlled by a program previously set up to control stroke, feed, and cutting speed

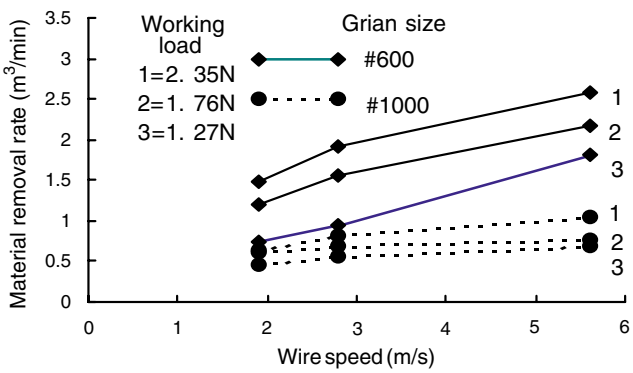

Fig. 3 Comparison of material removal rate for grain sizes #600 and #1000

Table 2 Experimental results for material removal rate and S/N ratio

Experiment no.	Control factors				Material removal rate (mm^2/min)			S/N (dB)
	θ	C	G	U	1	2	3	
1	1	1	1	1	1.115	1.098	1.165	1.023
2	1	2	2	2	2.643	2.663	2.700	8.525
3	1	3	3	3	3.793	3.205	2.767	10.037
4	2	1	1	2	2.013	1.702	1.447	4.479
5	2	2	2	3	3.232	3.613	3.323	10.573
6	2	3	3	1	3.863	3.765	4.022	11.774
7	3	1	2	1	2.160	1.703	2.147	5.872
8	3	2	3	2	3.285	3.732	3.272	10.657
9	3	3	1	3	3.812	3.920	3.952	11.806
10	1	1	3	3	1.460	1.395	1.663	3.485
11	1	2	1	1	1.613	1.982	2.005	5.289
12	1	3	2	2	2.720	2.983	2.910	9.141
13	2	1	2	3	1.905	1.665	2.315	5.618
14	2	2	3	1	3.310	3.197	3.798	10.648
15	2	3	1	2	4.010	3.278	4.048	11.421
16	3	1	3	2	1.590	2.058	2.222	5.559
17	3	2	1	3	3.373	3.423	3.560	10.755
18	3	3	2	1	3.678	3.802	3.750	11.463

of the steel wire and to carry free abrasives. In the swinging case (*2* in Fig. 1), the time required for grains to enter and exit the cutting zone is short, and chip disposal is smooth. Thus, the wire saw combined with swinging generates a high material removal rate. The angle of the swinging steel wire and reciprocating speed can be programmed by users. The steel wire can be made of stainless steel or other materials such as tungsten.

The *6* in Fig. 1 is the Z-axis platform. This platform consists of a precision screw, step motor, and decelerator. A computer program is utilized for step motor control and drives the precision screw through the deceleration mechanism. The Z-axial platform drives the fixture slightly upward, thereby feeding the workpiece toward the steel wire; the wire saw machining process is then complete. Figure 2 shows the X-axial platform and fixture

Table 3 Analysis of variance response table for material removal rate

Factor	Degree of freedom (F)	Sum of square (SS)	Variance (V)	F_0	$F_{0.05\cdot v1.v2}$
θ	2	35.4709	17.7354	50.7172	4.46
C	2	143.2256	71.6128	204.7876	4.46
G	2	5.3734	2.6867	7.6830	4.46
U	2	3.2508	1.6254	4.6481	4.46
Error	9	3.1472	0.3497		4.46
Total	17	190.4679			

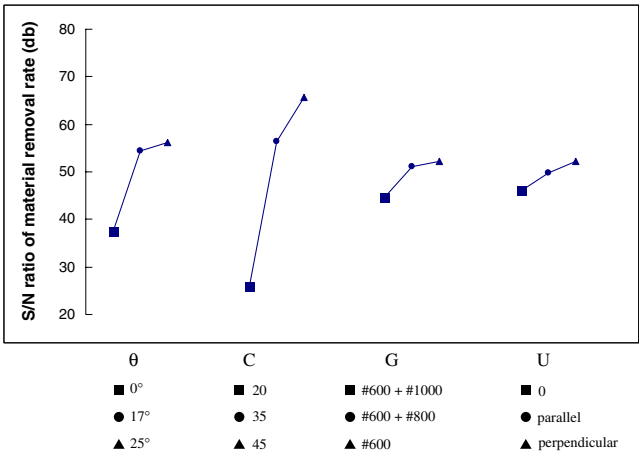

Fig. 4 S/N graph for material removal rate

mechanism (*4* and *5* in Fig. 1). The fixture can be replaced to meet cutting requirements, and uses the ultrasonic vibration-aid.

Taguchi approach is a powerful design tool for high-quality systems [8]. The L18 orthogonal table in Taguchi quality design is employed to determine the significant machining factors for experimental efficiency enhancement. All experimental factor settings (swinging angle (è), concentration (C), mixed grain (G) and ultrasonic direction (U)) used in this experiment are shown in Table 1. Slurry concentration is a percentage of slurry grain weight (weight of grain/weight of slurry as a whole). This study uses ultrasonic vibrations parallel to the feed (parallel to the Z-axis in Fig. 1) and perpendicular to the feed (perpendicular to the Z-axis in Fig. 1).

Material removal rate becomes extremely small (Fig. 3) when only fine grains exist in the slurry (e.g., only #1000 grains). Grain suspension in the slurry is difficult when only large grains (for example #300) are used. The wire has

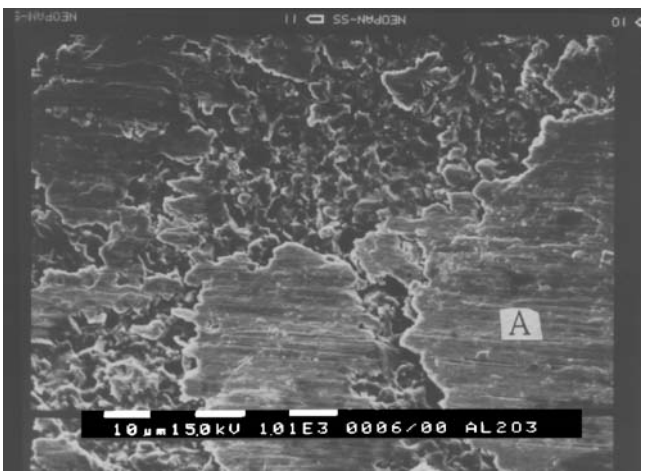

Fig. 5 SEM photo of Al_2O_3 without slurry

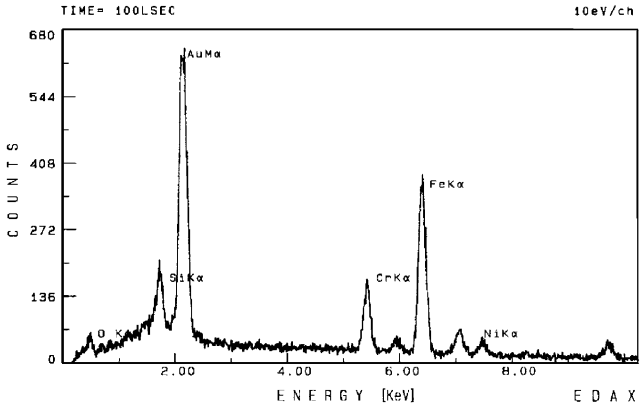

Fig. 6 The energy-dispersive spectrometer (EDS) for point A

difficulty bringing such large slurry grains into the cutting zone, causing poor machining efficiency.

3 Experimental results and data analysis

3.1 Analysis of S/N ratio

The Taguchi approach is employed for experimental plan development. The method employs a generic signal-to-noise (S/N) ratio to quantify present variation. The machining characteristics measured in this study include material removal rate, machined surface roughness of wafers, kerf width, steel wire wear, and flatness. The material removal rate represents machining efficiency. Thus, a high value is positively correlated as better, or the higher-is-better (HB) characteristic. Machined wafer surface roughness is a surface smoothness index. Kerf width and flatness denote machining precision, whereas steel wire wear indicates steel wire life. In order to eliminate the experimental error, the wire saw machining test was repeated three times at each condition. The goal is to minimize the values, thus called the lower-is-better (LB) characteristic. The S/N ratios are calculated using the following equations [9]:

$$\eta = 10\log\left(\frac{S}{N}ratio\right) \tag{1}$$

$$\text{HB}: \left(\frac{S}{N}ratio\right) = \frac{1}{\sigma_{HB}{}^2} \quad \sigma_{HB}{}^2 = \frac{1}{n}\left(\frac{1}{y_1{}^2} + \frac{1}{y_2{}^2} + \ldots.. + \frac{1}{y_n{}^2}\right) \tag{2}$$

$$LB: \left(\frac{S}{N}ratio\right) = \frac{1}{\sigma_{LB}{}^2} \quad \sigma_{LB}{}^2 = \frac{1}{n}\left(y_1{}^2 + y_2{}^2 + \ldots. + y_n{}^2\right) \tag{3}$$

Table 4 Experimental results for wafer surface roughness and S/N ratio

Experiment no.	Control factors				Wafer roughness (μm)			S/N (dB)
	θ	C	G	U	1	2	3	
1	1	1	1	1	0.45	0.54	0.66	5.088
2	1	2	2	2	0.43	0.56	0.49	6.087
3	1	3	3	3	0.43	0.57	0.60	5.377
4	2	1	1	2	0.54	0.59	0.58	4.876
5	2	2	2	3	0.48	0.35	0.51	6.897
6	2	3	3	1	0.42	0.41	0.37	7.946
7	3	1	2	1	0.31	0.48	0.36	8.181
8	3	2	3	2	0.49	0.42	0.44	6.917
9	3	3	1	3	0.51	0.58	0.59	5.019
10	1	1	3	3	0.42	0.46	0.54	6.449
11	1	2	1	1	0.62	0.65	0.63	3.966
12	1	3	2	2	0.38	0.35	0.43	8.222
13	2	1	2	3	0.47	0.48	0.48	6.435
14	2	2	3	1	0.49	0.34	0.46	7.233
15	2	3	1	2	0.38	0.38	0.47	7.698
16	3	1	3	2	0.32	0.48	0.49	7.190
17	3	2	1	3	0.38	0.49	0.37	7.600
18	3	3	2	1	0.40	0.46	0.38	7.645

Table 5 Analysis of variance response table for wafer surface roughness

Factor	Degree of freedom (F)	Sum of square (SS)	Variance (V)	F_0	$F_{0.05\cdot v1.v2}$
θ	2	5.0636	2.5318	1.7918	4.46
C	2	1.3397	0.6698	0.4741	4.46
G	2	7.6499	3.8249	2.7071	4.46
U	2	0.9119	0.4560	0.3227	4.46
Error	9	12.7165	1.4129		
Total	17	27.6816			

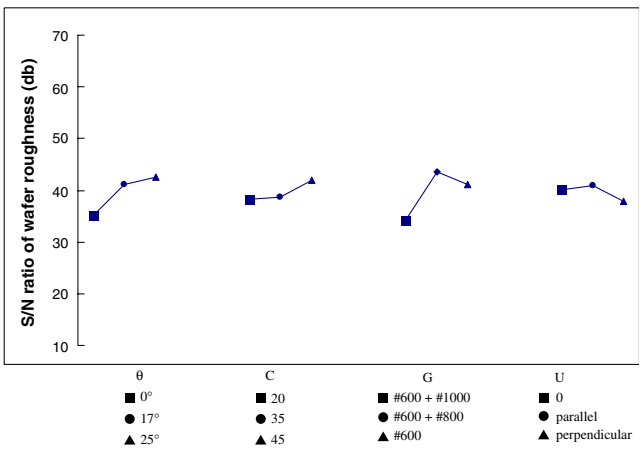

Fig. 7 S/N graph for wafer surface roughness

where η is the observed value, i.e., the calculated value of the S/N ratio (unit: dB), y_n is the observed value and n is the repeated number.

3.2 Analysis of variance

The ANOVA and F-test are applied to analyze the experimental data as follows [9]:

$$S_m = \frac{(\sum \eta_i)^2}{18}, \quad S_T = \sum {\eta_i}^2 - S_m \tag{4}$$

$$S_A = \frac{(\sum {\eta_{Ai}}^2)^2}{N} - S_m, \quad S_E = S_T - \sum S_A \tag{5}$$

$$V_A = \frac{S_A}{f_A}, \quad F_{Ao} = \frac{V_A}{V_E} \tag{6}$$

where S_T is the sum of squares due to total variation, S_m is the sum of squares due to the means, S_A is the sum of squares due to parameter A (A=θ, C, G, U), S_E is the sum of squares due to error, η_i is the η value of each experiment (i=1....18), η_{Ai} is the sum of the i level of parameter A (i=1, 2 or i=1, 2, 3), N is the repeating number of each level of parameter A, f_A is the degree of freedom of parameter A, V_A is the variance of parameter A, and F_{Ao} is the F-test value of parameter A.

Table 6 Experimental results for steel wire wear and S/N ratio

Experiment no.	Control factors				Steel wire wear (μm)			S/N (dB)
	θ	C	G	U	1	2	3	
1	1	1	1	1	0.90	0.90	0.60	1.805
2	1	2	2	2	1.40	2.10	1.80	−5.056
3	1	3	3	3	1.10	1.40	1.60	−2.810
4	2	1	1	2	4.40	4.10	3.50	−12.079
5	2	2	2	3	1.10	1.10	0.60	0.331
6	2	3	3	1	1.20	1.40	1.60	−2.981
7	3	1	2	1	3.10	3.30	2.70	−9.668
8	3	2	3	2	2.00	1.60	1.60	−4.829
9	3	3	1	3	1.60	1.20	0.90	−2.050
10	1	1	3	3	2.20	1.60	1.30	−4.814
11	1	2	1	1	1.20	1.30	2.10	−4.003
12	1	3	2	2	1.00	0.80	0.50	2.007
13	2	1	2	3	2.30	2.00	2.40	−7.004
14	2	2	3	1	3.40	3.60	4.20	−11.478
15	2	3	1	2	3.60	4.10	3.80	−11.684
16	3	1	3	2	2.80	3.60	2.10	−9.245
17	3	2	1	3	1.90	2.60	2.20	−7.050
18	3	3	2	1	1.60	1.90	1.90	−5.132

Table 7 Analysis of variance response table for steel wire wear

Factor	Degree of freedom (F)	Sum of square (SS)	Variance (V)	F_0	$F_{0.05\cdot v1.v2}$
θ	2	94.6253	47.3126	2.6055	4.46
C	2	28.0691	14.0345	0.7729	4.46
G	2	13.7556	6.8778	0.3788	4.46
U	2	25.5380	12.7690	0.7032	4.46
Error	9	163.4313	18.1590		
Total	17	325.4193			

3.3 Experimental results and analysis

Table 2 shows experimental results for material removal rate and corresponding S/N ratios obtained using Eqs. (1) and (3). Table 3 presents ANOVA results for material removal rate and Fig. 4 shows the S/N response graph for material removal rate. The data reveals that with wire swinging, the time required for grains to enter and exit the cutting zone is short and the chip disposal increases efficiency, generating a high material removal rate. An increase in slurry concentration increases the amount of active grains, thereby increasing the material removal rate. Grain sizes used are #600+#1000, #600+#800 and #600. The effect of wire saw machining on material removal rate is insignificant as all three levels include the #600 size. Furthermore, wire saw machining improves the material removal rate with the aid of ultrasonic.

Figure 5 shows the SEM microphotography of Al_2O_3 when operated without slurry. The energy-dispersive spectrometer (EDS) for point A (Fig. 6) show the

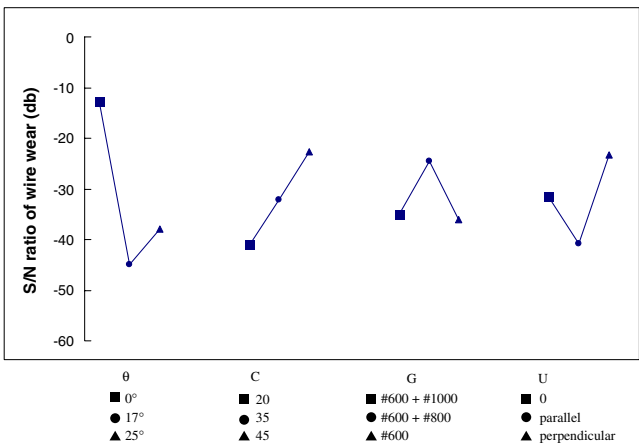

Fig. 8 S/N graph for steel wire wear

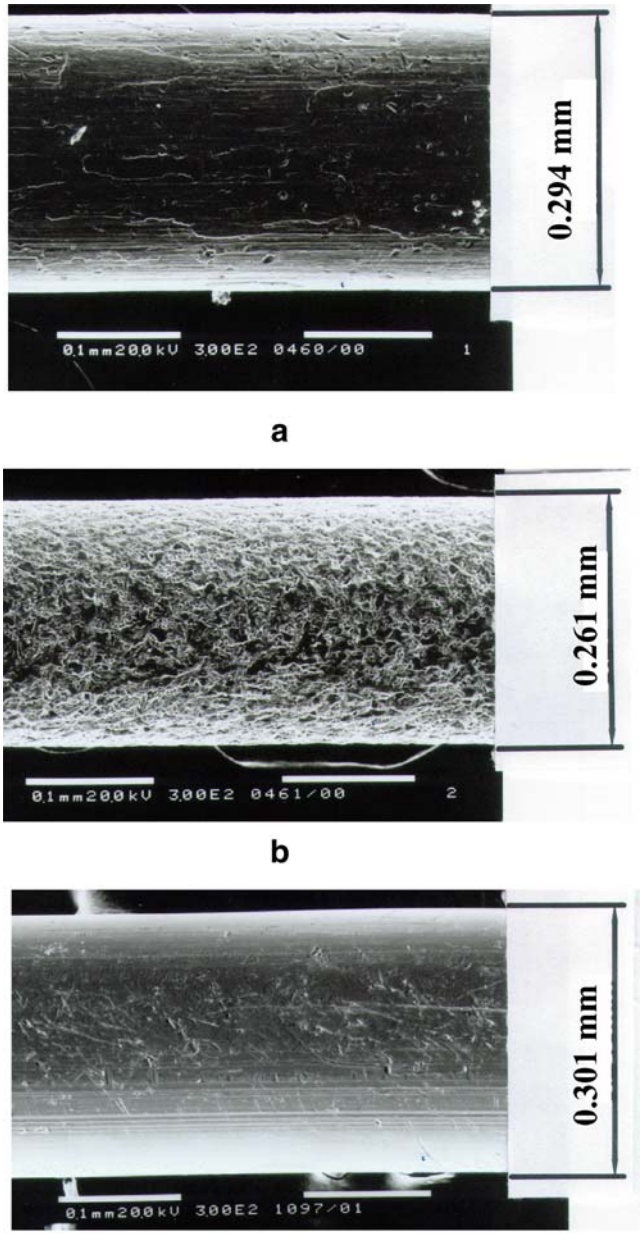

Fig. 9 Steel wire wear in SEM photo: **a** Without slurry; **b** With slurry (Gc+water); **c** Steel wire before use

microstructure of stainless steel, containing Fe, Cr, Ni, and Si. The wire has no machining capability due to the absence of slurry and, thus, is welded onto the workpiece surface.

Table 4 shows the experimental results for wafer surface roughness and the corresponding S/N ratios. Table 5 lists ANOVA results for wafer surface roughness. Figure 7 presents the S/N response graph for wafer surface roughness. Cutting amount by each grain in the cutting zone is extremely small during wire saw machining, similar to that in the polishing process. Thus, mixed #600+# 800 grains with wire swinging produce good surface roughness.

Table 8 Experimental results for kerf width and S/N ratio

Experiment no.	Control factors				Kerf width (mm)			S/N (dB)
	θ	C	G	U	1	2	3	
1	1	1	1	1	0.355	0.351	0.355	9.028
2	1	2	2	2	0.351	0.360	0.357	8.969
3	1	3	3	3	0.368	0.363	0.363	8.766
4	2	1	1	2	0.369	0.362	0.367	8.736
5	2	2	2	3	0.354	0.359	0.362	8.911
6	2	3	3	1	0.355	0.358	0.361	8.922
7	3	1	2	1	0.362	0.366	0.365	8.770
8	3	2	3	2	0.366	0.362	0.355	8.849
9	3	3	1	3	0.368	0.373	0.362	8.690
10	1	1	3	3	0.355	0.351	0.349	9.077
11	1	2	1	1	0.357	0.355	0.350	9.020
12	1	3	2	2	0.356	0.347	0.354	9.060
13	2	1	2	3	0.368	0.355	0.365	8.809
14	2	2	3	1	0.367	0.353	0.378	8.731
15	2	3	1	2	0.352	0.361	0.360	8.933
16	3	1	3	2	0.366	0.368	0.371	8.675
17	3	2	1	3	0.367	0.360	0.353	8.873
18	3	3	2	1	0.364	0.355	0.351	8.953

Table 6 shows the experimental results for steel wire wear and the corresponding S/N ratios. Table 7 lists the ANOVA results for the wear of steel wire. Figure 8 shows the S/N response graph for the wear of steel wire. Material removal rate is approximately proportional to steel wire wear. Figure 9a and b show the result of steel wire wear under the same cutting conditions. Figure 9a, operated without slurry, shows moderate wire damage, and, thus, limited steel wire wear (diameter of the wire is 0.294 mm). However, workpiece material removal rate is almost zero in this case. Figure 9b with slurry clearly shows excessive abrasion of the wire by grains, resulting in considerable wear (diameter of the wire is 0.261 mm). Figure 9c presents the steel wire before use.

Table 9 Analysis of variance response table for kerf width

Factor	Degree of freedom (F)	Sum of square (SS)	Variance (V)	F_0	$F_{0.05,v1,v2}$
θ	2	0.114	0.057	3.735	4.46
C	2	0.007	0.003	0.218	4.46
G	2	0.017	0.009	0.561	4.46
U	2	0.008	0.004	0.252	4.46
Error	9	0.138	0.015		
Total	17	0.284			

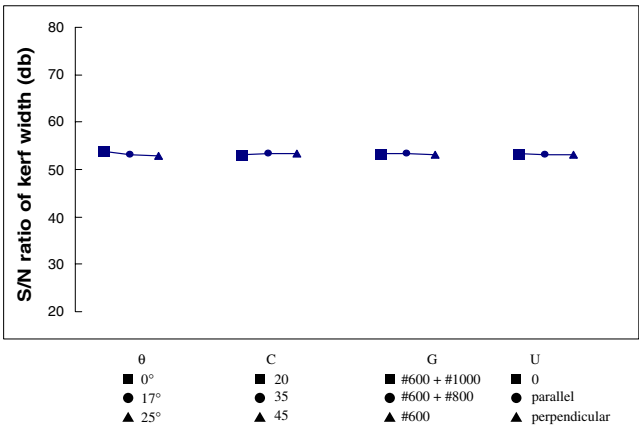

Fig. 10 S/N graph for kerf width

Table 8 presents the experimental results for kerf width and the corresponding S/N ratios. Table 9 lists the ANOVA results for kerf width. Figure 10 shows the S/N response graph for kerf width. Machining parameters do not have a significant effect on kerf width.

Table 10 shows the experimental results for flatness and the corresponding S/N ratios. Table 11 lists the ANOVA results for flatness. Figure 11 presents the S/N response graph for flatness. The machining parameters do not have any significant effect on flatness. Figure 12 shows that there is no corner chipping during wire saw machining. Figure 13 presents the SEM observations of subsurface regions of Al_2O_3 following wire saw machining which shows no microcracking exists.

Table 10 Experimental results for flatness and S/N ratio

Experiment no.	Control factors				Flatness (μm)			S/N (dB)
	θ	C	G	U	1	2	3	
1	1	1	1	1	7.01	7.67	6.73	−17.083
2	1	2	2	2	6.30	6.93	6.70	−16.454
3	1	3	3	3	6.71	6.68	6.55	−16.453
4	2	1	1	2	6.98	6.67	7.31	−16.891
5	2	2	2	3	5.43	7.20	7.47	−16.600
6	2	3	3	1	7.53	7.44	7.28	−17.405
7	3	1	2	1	6.39	6.01	6.50	−15.992
8	3	2	3	2	6.97	7.32	7.31	−17.149
9	3	3	1	3	7.29	7.86	7.76	−17.663
10	1	1	3	3	7.73	7.43	7.09	−17.410
11	1	2	1	1	7.16	7.20	6.86	−16.994
12	1	3	2	2	7.58	7.52	7.96	−17.718
13	2	1	2	3	6.02	6.33	6.12	−15.789
14	2	2	3	1	6.82	6.75	7.02	−16.732
15	2	3	1	2	7.69	7.85	7.96	−17.880
16	3	1	3	2	7.04	6.68	7.10	−16.830
17	3	2	1	3	7.15	7.33	7.36	−17.243
18	3	3	2	1	8.28	8.51	8.59	−18.548

Table 11 Analysis of variance response table for flatness

Factor	Degree of freedom (F)	Sum of square (SS)	Variance (V)	F_0	$F_{0.05 \cdot v1.v2}$
θ	2	0.3844	0.1922	0.4852	4.46
C	2	2.9854	1.4927	3.7683	4.46
G	2	0.6095	0.3047	0.7693	4.46
U	2	0.3165	0.1583	0.3995	4.46
Error	9	3.5651	0.3961		
Total	17	7.8609			

3.4 Gray relational analysis

Grey relational analysis can effectively be recommended as a method for optimizing the complicated inter-relationships among multiple performance characteristics [10–12]. Through the grey relational analysis, a grey relational grade is obtained to evaluate the multiple performance characteristics. As a result, optimization of the complicated multiple performance characteristics can be converted into the optimization of a single grey relational grade. The grey relational analysis first performs data preprocessing to normalize raw data for analysis. A linear normalization of S/N ratios is performed in the range between zero and unity, called grey relational generating. Grey relational analysis based on grey relational generating can effectively solve complicated interrelationships among multiple

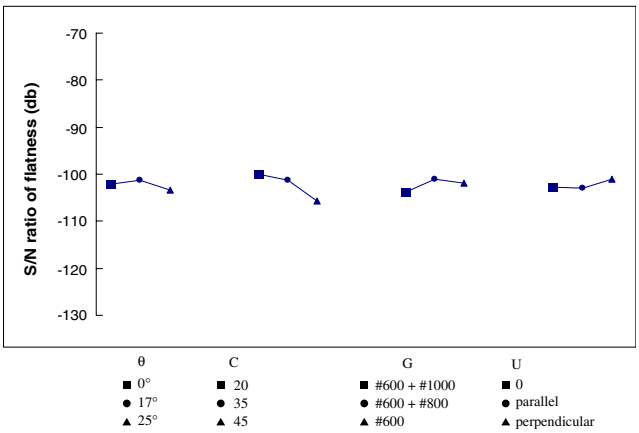

Fig. 11 S/N graph for flatness

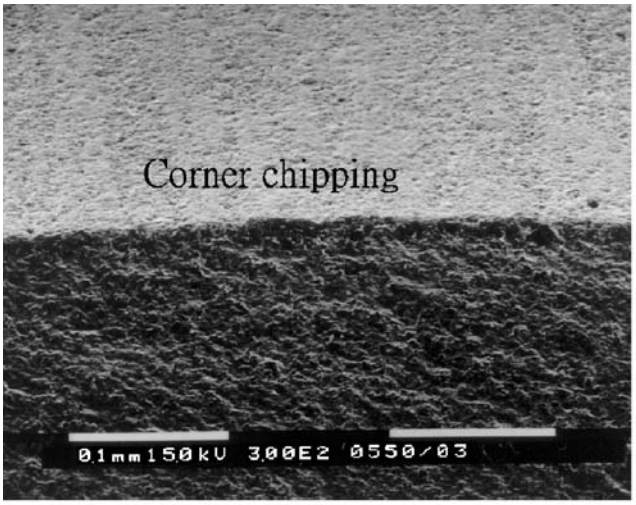

Fig. 12 No corner chipping during wire saw machining

performance characteristics [13]. The grey relational coefficient is [14]:

$$r(x_o(k),x_i(k)) = \frac{\min\limits_i \min\limits_k |x_0(k)-x_i(k)| + \zeta \max\limits_i \max\limits_k |x_0(k)-x_i(k)|}{|x_0(k)-x_i(k)| + \zeta \max\limits_i \max\limits_k |x_0(k)-x_i(k)|} \tag{7}$$

where $x_i(k)$ is the normalized value of the kth performance characteristic in the ith experiment, ζ is the distinguishing coefficient, $\zeta \in [0,1]$. The value of ζ can be adjusted according to actual system requirements. Wire saw machining parameters in this study have equal weighting; therefore, ζ is 0.5.

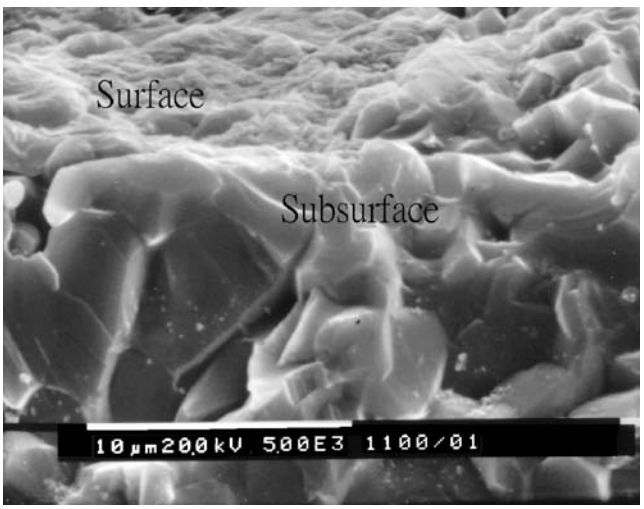

Fig. 13 Observations of subsurface regions with wire saw machining

Table 12 Grey relational grade and its order in the optimization process

Experiment	Grey relational grade	Order
1	0.6177	7
2	0.6082	10
3	0.5920	13
4	0.4145	18
5	0.7076	3
6	0.7277	2
7	0.6250	5
8	0.6046	11
9	0.5941	12
10	0.6120	9
11	0.5511	16
12	0.7809	1
13	0.5890	14
14	0.5638	15
15	0.6161	8
16	0.5024	17
17	0.6189	6
18	0.6552	4

The grey relational grade is a weighted sum of the grey relational coefficient, defined as [14]:

$$r(x_0,x_i) = \frac{1}{n}\sum_{k=1}^{n} r(x_0(k),x_i(k)) \tag{8}$$

where n is the number of performance characteristic. The grey relational grade shows the correlation between the reference sequence and the comparability sequence to be compared to. The evaluated grey relational grade fluctuates from 0 to 1 and equals one if these two sequences are identically coincident. Based on Eqs. (7) and (8), Table 12 presents the grey relational grade for each experiment using the L_{18} orthogonal array. Table 13 presents a summary of

Table 13 Grey relational grade and its order for each level of wire saw machining

Experiment	Grey relational grade	Order
θ1	0.6513	2
θ2	0.6656	1
θ3	0.6241	3
C1	0.4667	3
C2	0.6624	2
C3	0.8212	1
G1	0.3721	3
G2	0.8991	1
G3	0.6182	2
U1	0.5426	2
U2	0.4973	3
U3	0.7333	1

Table 14 Multiple performance characteristics with initial and optimal predicted wire saw machining parameters

Characteristic	Optimum wire saw machining parameters
Initial process parameters	θ1 C3 G2 U2
Grey theory prediction design	θ2 C3 G2 U3

the grey relational grade values for each level of wire saw machining parameters. Table 14 shows the performance characteristics with initial and optimal predicted wire saw machining parameters.

3.5 Verification tests

Once optimal wire saw machining parameters are selected, the final step predicts and verifies the performance improvement using optimal wire saw machining parameters. Table 15 presents the wire saw machining results for multiple performance characteristics. Comparing the grey theory prediction design (θ2 C3 G2 U3) with initial process parameters (θ1 C3 G2 U2) indicates that the material removal rate increases from 2.972 to 3.324 mm^2/min, wafer surface roughness decreases from 0.37 to 0.34 μm, steel wire wear decreases from 0.78 to 0.77 μm, kerf width decreases from 0.352 to 0.350 mm, and flatness decreases from 7.51 to 7.22 μm.

4 Conclusions

This study applies the grey relational analysis and Taguchi method to optimize the machining parameters with multiple performance characteristics (large material removal rate, low wafer surface roughness, small steel wire wear, low kerf width and flatness) after wire saw machining. Experimental results indicated that grey relational analysis could integrate the issues of multiple quality characteristics to obtain the optimal combination parameters in wire saw machining based on the concept of Taguchi method. As a result, the material removal rate increases from 2.972 to 3.324 mm^2/min, wafer surface roughness decreases from 0.37 to 0.34 μm, steel wire wear decreases from 0.78 to 0.77 μm, kerf width decreases from 0.352 to 0.350 mm, and flatness decreases from 7.51 to 7.22 μm. The successful uses of multiple performance characteristics can propose a comparatively objective methodology for those who engage in the design of experiment.

Table 15 Confirmation test results for multiple performance characteristics for wire saw machining

Material removal rate	Surface roughness of wafer	Steel wire wear	Kerf width	Flatness
Initial process parameters θ1 C3 G2 U2				
2.972 mm^2/min	0.37 μm	0.78 μm	0.352 mm	7.51 μm
Grey theory prediction design θ2 C3 G2 U3				
3.324 mm^2/min	0.34 μm	0.77 μm	0.350 mm	7.22 μm

Acknowledgment The authors wish to thank the Ministry of Education of the Republic of China, Taiwan, for financial support of this research.

References

1. Hsu CY (2000) The study of wire saw machining (in Chinese). Doctoral Thesis University of Taiwan
2. Bhagavat S, Kao I (2006) Theoretical analysis on the effects of crystal anisotropy on wiresawing process and application to wafer slicing. Int J Mach Tools Manuf 46(5):531–541
3. Yamamoto T (1995) Multi-wire slabbing of granite. Ind Diam Rev 55(567):179–181
4. Contardi GL (1993) Wire saw beads economic production. Ind Diam Rev 53(558):256–260
5. Kojima M (1990) Development of new wafer slicing equipment. Sumitomo Met 42(4):218–224
6. Suwabe H, Ishikawa KI, Miyashita T (1997) A study of the processing characteristics of a swinging multi-wire saw-regarding the effects of slurry composition. Int Conf on Precision Eng 1:253–256
7. Clark WI, Shih AJ, Lemaster RL, McSpadden SB (2003) Fixed abrasive diamond wire machining, part II: experiment design and results. Int J Mach Tools Manuf 43:533–542
8. Phillip JR (1989) Taguchi techniques for quality engineering. McGraw-Hill, New York
9. Wang CC, Yan BH (2000) Blind-hole drilling of Al_2O_3/6061 Al composite using rotary electro-discharge machining. J Mater Process Technol 102:90–102
10. Lin JL, Lin CL (2002) The use of the orthogonal array with grey relational analysis to optimize the electrical discharge machining process with multiple performance characteristics. Inter J Mach Tools Manuf 42(2):237–244
11. Tosun N (2006) Determination of optimum parameters for multi-performance characteristics in drilling by using grey relational analysis. Int J Adv Manuf Technol 28:450–455
12. Chang CK, Lu HS (2007) Design optimization of cutting parameters for side milling operations with multiple performance characteristics. Int J Adv Manuf Technol 32:18–26
13. Tarng YS, Juang SC, Chang CH (2006) The use of grey-based Taguchi methods to determine submerged arc welding process parameters in hardfacing. J Mater Process Technol 128:1–6
14. Deng JL (1992) The essential method of grey systems. HUST Press, Wuhan, China